Journal of Applied Polymer Science

Mechanical and Thermal Properties of Thermoplastic Random Copolyesters Made from Lipid-Derived Medium and Long Chain Poly(ω-hydroxyfatty acid)s

Jesmy Jose,[1,2] Shaojun Li,[1,2] Laziz Bouzidi,[1,2] Alcides Lopes Leao,[3] Suresh S. Narine[1,2]

[1]Department of Physics and Astronomy, Trent Centre for Biomaterials Research, Trent University, Peterborough, Ontario K9J 7B8, Canada

[2]Department of Chemistry, Trent Centre for Biomaterials Research, Peterborough, Ontario K9J 7B8, Canada

[3]Department of Natural Sciences, College of Agricultural Sciences, São Paulo State University (UNESP), Botucatu, Brazil

Correspondence to: S. S. Narine (E-mail: sureshnarine@trentu.ca)

ABSTRACT: The physical properties of novel thermoplastic random copolyesters [-$(CH_2)_n$-COO-/-$(CH_2)_n$-COO-]$_x$ made of long ($n = 12$) and medium ($n = 8$) chain length ω-hydroxyfatty esters [HO-$(CH_2)_n$-$COOCH_3$] derived from bio-based vegetable oil feedstock are described. Poly(ω-hydroxy tridecanoate/ω-hydroxy nonanoate) P(−Me13−/−Me9−) random copolyesters ($M_n = 11{,}000$–$18{,}500$ g/mol) with varying molar ratios were examined by TGA, DSC, DMA and tensile analysis, and WAXD. For the whole range of P(−Me13−/−Me9−) compositions, the WAXD data indicated an orthorhombic polyethylene-like crystal packing. Their melting characteristics, determined by DSC, varied with composition suggesting an isomorphic cocrystallization behavior. TGA of the P(−Me13−/−Me9−)s indicated improved thermal stability determined by their molar compositions. The glass transition temperature, investigated by DMA, was also found to vary with composition. The crystallinities of P(−Me13−/−Me9−)s however, were unaffected by the composition. The stiffness (Young's modulus) of these materials was found to be related to their degrees of crystallinity. © 2014 Wiley Periodicals, Inc. J. Appl. Polym. Sci. **2014**, *131*, 40492.

KEYWORDS: biopolymers and renewable polymers; copolymers; polyesters; structure–property relations; thermoplastics

Received 7 October 2013; accepted 21 January 2014

DOI: 10.1002/app.40492

INTRODUCTION

Poly(hydroxy acid)s [-$(CH_2)_n$-COO-]$_x$ are an interesting class of biodegradable thermoplastic polyesters that are widely researched for drug delivery and tissue engineering applications.[1,2] Various short [e.g., poly (glycolic acid),[3] PGA ($n = 1$), poly(3-hydroxy propionic acid),[4] P3HA, ($n = 2$)], medium [e.g., poly(ε-caprolactone),[5] PCL ($n = 5$)] and long chain [e.g., poly(15-pentadecalactone),[6] PPDL($n = 14$)] poly(hydroxy acid) homologues have been synthesized and were shown to exhibit distinctive physiochemical properties determined by their chemical structures.

Recently, medium and long chain poly (hydroxy acid)s derived from vegetable oils have received much attention as potential substitutes for petroleum-derived polyesters.[7,8] The unsaturated long chain (16–22 carbons) fatty acids derived from triacylglyceride (TAG) molecules of vegetable oils can be chemically transformed to ω-hydroxyfatty acid monomers, which upon polymerization gives medium (e.g., poly(ω-hydroxynonanoate),[9,10] $n = 9$) and long chain poly(ω-hydroxyfatty acid)s [-$(CH_2)_n$-COO-]$_x$ (e.g., poly(ω - hydroxytridecanoate),[10] $n = 12$, poly(ω-hydroxyoctadecanoate),[10] $n = 17$). These polyesters crystallize into polyethylene (PE)-like orthorhombic crystal lattices.[11] Their physical properties such as thermal, mechanical properties, etc. varies as a function of both their molecular chain lengths as well as the chemical structure of the repeating [-$(CH_2)_n$-COO-] monomer units.[11]

Copolymerization is well known as a convenient way for adjusting physiochemical properties through the composition and constitution of copolyesters.[8,12–14] For vast majority of aliphatic A/B copolyesters where both the A and B components are crystallisable, but not often compatible, the degree of crystallinity decreases with increasing amount of the minor component. As a result, the A/B copolyesters often become totally amorphous even at low comonomer content. For poly(hydroxy acid)s, however, the similarity in chemical structure presents potential copolyester systems [-$(CH_2)_n$-COO-/-$(CH_2)_n$-COO-]$_x$ capable of cocrystallization whereby the thermal and mechanical properties

Additional Supporting Information may be found in the online version of this article.

Table I. Chemical Name and Structures of Omega-Hydroxyfatty Ester Monomers, Homopolymers, and Copolyesters

Chemical name	Chemical structure	Abbreviation
Methyl 9-hydroxynonanoate	HO-$(CH_2)_8$-$COOCH_3$	Me-ω-OHC9
Methyl 13-hydroxytridecanoate	HO-$(CH_2)_{12}$-$COOCH_3$	Me-ω-OHC13
Poly(methyl ω-hydroxynonanoate)	[-$(CH_2)_8$-COO-]$_x$	Me13
Poly(methyl ω-hydroxytridecanoate)	[-$(CH_2)_{12}$-COO-]$_y$	Me9
Poly(ω-hydroxy tridecanoate/ω-hydroxy nonanoate)	[(-$(CH_2)_{12}$-COO-)$_x$/(-$(CH_2)_8$-COO-)$_y$]$_Z$	P(−Me13−/−Me9−)

of the copolymers can be controlled without significant loss of crystillinity. A few of the nonrenewable poly(hydroxy acid) copolyesters [-$(CH_2)_n$-COO-/-$(CH_2)_n$-COO-]$_x$ prepared so far by chemical means are poly (glycolide/ε-caprolactone)[15] [-(CH_2)-COO-/-$(CH_2)_5$-COO-]$_x$, and poly (ε-caprolactone/ω-pentadecalactone)[16] [-$(CH_2)_5$-COO-/-$(CH_2)_{14}$-COO-]$_x$. To the best of our knowledge, no poly(hydroxy acid) based copolyesters have been prepared from renewable sources.

This study focussed on the solid-state characterization of Poly(ω-hydroxy tridecanoate/ω-hydroxy nonanoate) [-$(CH_2)_{12}$-COO-/-$(CH_2)_8$-COO-]$_x$ thermoplastic random copolyesters derived from vegetable oil using WAXD, TGA, DSC, DMA, and tensile analysis. The melting, glass transition and thermal decomposition properties of Poly(ω-hydroxy tridecanoate/ω-hydroxy nonanoate) P(−Me13−/−Me9−)s were to be found tuneable with the copolyester compositions. Interestingly, their crystallinities, and thereby the related mechanical properties were relatively unaffected by composition.

EXPERIMENTAL

The homopolymers poly(methyl ω-hydroxynonanoate), and poly(methyl ω-hydroxytridecanoate), and their copolyesters (P(−Me13−/−Me9−)) were prepared by the melt polycondensation of methyl 13-hydroxytridecanoate and methyl 9-hydroxynonanoate synthesized from mono-unsaturated fatty acids. The chemical structures of the monomers, homopolymers, and the copolyesters are listed in Table I. The synthesis and copolymerization procedures are detailed in a previous work.[10] Prior to the physical property measurements the copolyesters were first melted at 120°C and molded in to films on a Carver 12 ton hydraulic heated bench press (Model 3851-0, Wabash, IN) at a controlled cooling rate of 5°C/min. Table II summarizes the composition, weight average (M_w), number average (M_n) molecular weights, PDI, and concentration of ester groups (C_e) (wt%) calculated for the P(−Me13−/−Me9−) copolyester samples. The sample is labeled using an abbreviation for its methyl ω-hydroxytridecanoate comonomer (Me13) appended by its molar ratio, followed by its M_w in kg/mol. The homopolymers (Me13 and Me9) and the P(−Me13−/−Me9−) copolymers exhibited comparable molar masses in the range between 11,000 and 18,500 g/mol (M_n).

Characterization Techniques

Calorimetric studies were performed on a DSC Q200 (TA instrument, Newcastle, DE) following the ASTM D3418 standard procedure under a dry nitrogen gas atmosphere. The sample (5.0–6.0 mg) was first equilibrated at 0°C and heated to 120°C at a constant rate of 3.0°C/min (first heating cycle). The sample was held at that temperature for 10 min to erase the thermal history, then cooled down to −90°C with a cooling rate of 3°C/min (cooling cycle) and subsequently reheated to 120°C at the same rate (second heating cycle). During the second heating cycle, measurements were performed with modulation amplitude of 1°C/min and modulation period of 60 s.

Thermogravimetric Analysis was carried out using a TGA Q500 (TA instrument, Newcastle, DE) following the ASTM E2550-11 standard procedure. Samples of ~10 mg were heated from room temperature to 600°C under dry nitrogen at constant heating rates of 10°C/min.

Table II. Composition, Weight Average (M_w), Number Average (M_n) Molecular Weights, PDI, and Concentration of Ester Groups (C_e) (wt %) Calculated for P(−Me13−/−Me9−) Copolyesters

Sample code	Me-ω-OHC13/Me-ω-OHC9molar ratio[a]	M_w [b] (g/mol)	M_n [b] (g/mol)	PDI	C_e (wt %)
Me13-100(25k)	100 : 0	24,830	14,606	1.7	13
Me13-94(33k)	94 : 06	32,726	18,408	1.8	13
Me13-85(21k)	85 : 15	20,558	11,742	1.8	14
Me13-71(25k)	71 : 29	24,806	13,255	1.9	14
Me13-48(19k)	48 : 52	18,688	11,934	1.6	15
Me13-43(20k)	43 : 57	20,019	12,059	1.7	16
Me13-0(16k)	0 : 100	15,712	9,936	1.6	17

[a] From ^{1}H-NMR.
[b] From GPC.

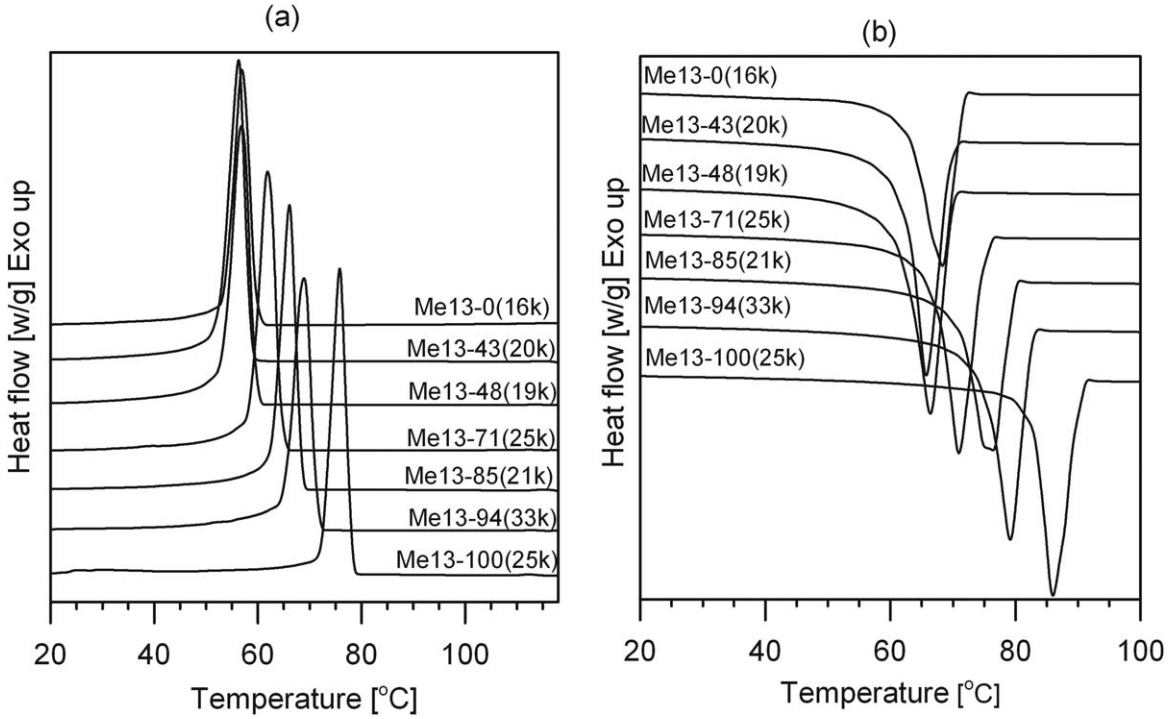

Figure 1. DSC (a) cooling and (b) heating thermograms of P(−Me13−/−Me9−) copolyesters.

Viscoelastic behavior of copolyesters was studied by performing dynamic temperature sweeps in a dynamic mechanical analyzer (TA instrument, DMA Q800) equipped with a liquid nitrogen cooling system. Rectangular polymer films (17.5 mm × 12 mm × 0.6 mm) were analyzed in a dual cantilever-bending mode following the ASTM E1640-09 standard procedure at a frequency of 1 Hz and fixed oscillation displacement of 15 μm. The samples were heated under a constant rate of 1°C/min over a temperature range of −90°C to 80°C.

The static mechanical properties of the synthesized polymer films were determined at room temperature using a Texture Analyser (Texture Technologies Corp, NJ) using the ASTM D882 procedure. The sample was stretched at a rate of 5 mm/min from a gauge of 35 mm.

Wide-angle X-ray diffraction (WAXD) was carried out at room temperature (~22°C) on an EMPYREAN diffractometer system (PANalytical, The Netherlands) equipped with a Cu-Kα radiation source ($\lambda = 1.540598$ Å) and a PIXcel-3D^{TM} area detector. The WAXD patterns were recorded at 45 kV and at 40 mA. The 2θ-scanning range was from 3° to 90°. Totally, 3313 points were collected in 45 min in this process. The data were processed and analyzed using the Panalytical's X'Pert HighScore V3.0 software. The degree of crystallinity was estimated according to a well-established procedure.[17] The percentage degree of crystallinity (X_c) is given by eq. (1),

$$X_C = 100 \times \frac{A_C}{A_C + A_A} \quad (1)$$

where A_c is the area under the resolved crystal diffraction peaks and A_A, the area of the amorphous contribution halo.

RESULTS AND DISCUSSION

Melt Transition Behavior of P(−Me13−/−Me9−) Copolyesters

The cooling and heating thermograms for the copolymer systems are shown in Figure 1(a,b). All samples exhibited sharp single melting and crystallization peaks, which may be a strong evidence of co-crystallization.[18,19] With increasing (Me-ω-OHC9) comonomer content, the melting and crystallization peaks [samples Me13–100(25 k) to Me13–43(20 k), Figure 1(a,b)] shifted to lower temperatures suggesting less stable crystals for P(−Me13−/−Me9−)s. The characteristic parameters obtained from DSC are summarized in Table III. The peak melting point (T_m) of P(−Me13−/−Me9−) copolyesters varied from 66 to 88°C for different molar compositions.

Figure 2 displays the composition dependence of T_m and peak crystallization temperature (T_c) for the copolyesters. Both T_m and T_c exhibited a minimum negative deviation from linear behavior of melting/crystallization point versus composition, and is indicative of an isomorphic cocrystallization behavior.[18,19] For P(−Me13−/−Me9−) samples (Me13–48(19k) and Me13–43(20k)) with around 50 : 50 ratio of (Me-ω-OHC13): (Me-ω-OHC9) comonomer units the melting point (T_m) varied only slightly (±5°C) from that of Me13 homopolymer (Figure 2).

Crystalline Structure of Copolyesters

Figure 3(a) shows the crystalline structures of Me13, Me9 homopolymers and P(−Me13−/−Me9−) copolymers investigated by wide-angle X-ray diffraction (WAXD). The analysis of the WAXD patterns was performed using a fitting module of

Table III. Characteristic Parameters of P(−Me13−/−Me9−) Copolymers Obtained by DSC and WAXD

	Cooling		Second melting			
Sample code	T_c (°C)	ΔH_c (J/g)	T_m (°C)	ΔH_c (J/g)	X_c (%)	$\Delta H_{m(cryst)}$ (J/$g_{(cryst)}$)
Me13-100(25k)	75.1	139	86.0	158	75	170
Me13-94(33k)	68.9	128	79.4	140	68	170
Me13-85(21k)	66.0	130	76.1	126	77	183
Me13-71(25k)	62.1	131	71.1	134	76	176
Me13-48(19k)	57.1	128	66.6	132	72	167
Me13-43(20k)	56.2	126	65.5	131	77	211
Me13-0(16k)	57.1	97	68.5	115	67	210

Peak temperature of crystallization, T_c, enthalpy of crystallization, ΔH_c obtained from cooling cycle, peak temperature of melting, T_m, enthalpy of melting, ΔH_m obtained from second heating cycle, degree of crystallinity, X_c, estimated from WAXD, and $\Delta H_{m(cryst)}$, the melting enthalpy per gram of the crystal phase. The uncertainties attached to the characteristic temperatures, enthalpies, and degree of crystallinity are better than 0.5°C, 8 J/g, and 5% respectively.

HighScore Version 3.0. The amorphous contribution was added in the form of two wide lines (centered at ~3.8 and 4.6 Å) as typically done for semicrystalline polymers.[17] The observed intensities were evaluated by integrating the crystalline peaks observed in the WAXD profiles. All samples [from Me13–100(25 k) to Me13-0(16 k)] exhibited sharp diffraction peaks over the entire copolymer composition range [Figure 3(a)]. The experimental WAXD profiles consisted of four resolved diffraction peaks which are characteristic of a large crystalline phase, superimposed to relatively small wide halos which are indicative of the presence of an amorphous phase. The homopolymers Me13–100(25 k) and Me13-0(16 k), as well as their copolyesters demonstrated similar WAXD spectra indicating that they crystallized in similar crystal forms. The sharp diffraction peaks observed in the WAXD patterns [Figure 3(a)] are characteristic of the common orthorhombic methylene subcell packing and are reminiscent of that obtained for melt crystallized polyethylene (PE).[20] The two very strong lines at positions 21.30–21.5° [2θ] and 23.89–24.02° [2θ] (d-spacings of 4.16 ± 0.02 Å and 3.74 ± 0.02 Å, respectively) originated from the 110 and 200 reflections of the orthorhombic symmetry, respectively. The weaker peaks at d-spacings of 2.99 ± 0.01 Å and 2.50± 0.02 Å originated from the 210 and 020 reflections of the orthorhombic symmetry, respectively.

The variation of the corresponding d-spacing of the crystal peaks with copolyester composition is demonstrated in Figure 3(b). For P(−Me13−/−Me9−) (Me13–94(33 k) to Me13–43(20 k)) the d-spacing changes in a linear continuous manner with increasing content of (Me-ω-OHC9) comonomer units. This is expected for isomorphic cocrystallized systems where the two homopolymer repeating units have similar crystal structures.[18,19] The close similarity of crystal symmetries for (Me-ω-OHC9) and (Me-ω-OHC13) induces P(−Me13−/−Me9−)s to adopt polyethylene-like crystal structures, in agreement with early observations for poly (ε-caprolactone/ω-pentadecalactone) [-$(CH_2)_5$-COO−/−$(CH_2)_{14}$-COO-]$_x$ random copolyesters, which also cocrystallize into a common crystal lattice.[16]

The degree of crystallinity, X_c estimated for the copolyesters were high, in the 68% to 77% range (Table III). Figure 4 displays the variation of X_c (estimated from WAXD) and ΔH_m (determined from DSC data) as a function of the composition (expressed on a weight basis since results from both techniques depend on the mass of analyzed sample). ΔH_m and X_c show very little variability with copolyester composition and indicates good crystallizing ability of P(−Me13−/−Me9−) copolyesters. The ratio of the ΔH_m (per gram of whole sample, from DSC) to the fractional crystallinity (X_c, from WAXD) represents the melting enthalpy per gram of the crystal phase, and is listed in Table III. The enthalpy of fusion of P(−Me13−/−Me9−) crystals tends to decrease with increasing (Me-ω-OHC9) comonomer content, which is attributable to the inclusion of (Me-ω-OHC9) units in the (Me-ω-OHC13) lattice.

Thermal Stabilities of P(−Me13−/−Me9−) Copolyesters

The TGA derivative (DTG) of the homopolymers (Me13–100(25 k) and Me13-0(16 k)) as well as the P(−Me13−/−Me9−) copolymers (Me13–94(33 k) to Me13–43(20 k)) displayed (Figure 5) a single prominent peak indicative of a single step degradation process

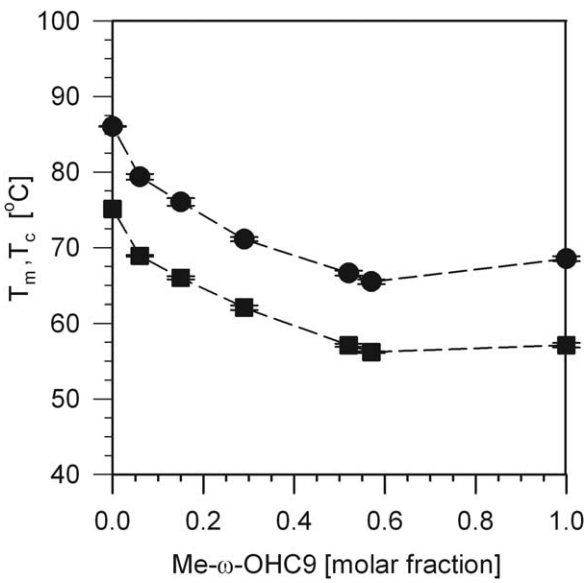

Figure 2. Composition dependence of the melting temperature (T_m) (●) and melt crystallization temperature (T_c) (■) of P(−Me13−/−Me9−) copolysters. The dotted lines are guidelines for eyes.

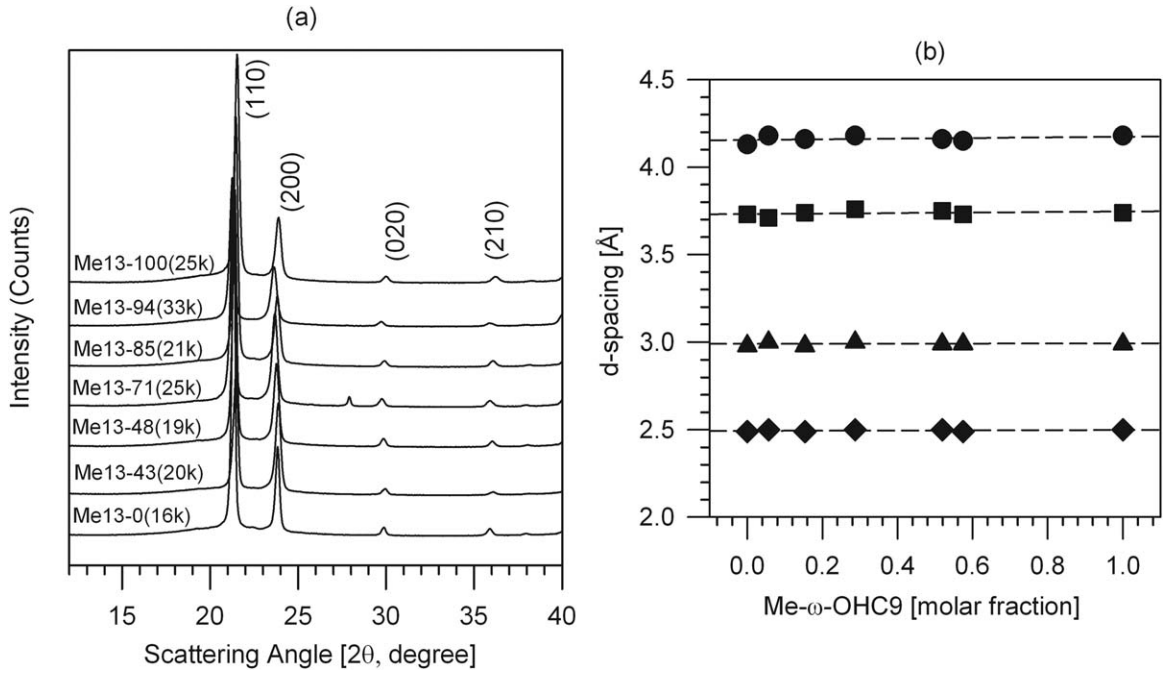

Figure 3. (a) WAXD patterns taken at room temperature for P(−Me13−/−Me9−) copolymers and (b) Changes of *d*-spacing for P(−Me13−/−Me9−) copolymers as a function of Me-*ω*-OHC9 (molar fraction).

initiated by the random scission of the ester linkage at the alkyl-oxygen bonds at temperatures around 340–460°C.[21]

The onset degradation temperature, defined at 5% weight loss ($T_{d(5)}$), and $T_{d(\max)}$ the temperature at maximum degradation rate are listed in Table IV. $T_{d(5)}$ is a direct measure of thermal stability, and is a crucial parameter for the melt-processing of thermoplastics. The noticeable effects of copolymer composition on $T_{d(5)}$ and $T_{d(\max)}$ are shown by Figure 6. P(−Me13−/−Me9−)s (Me13–94(33 k) to Me13–43(20 k)) exhibited a positive deviation from linear behavior of $T_{d(5)}$ versus composition (Figure 6) with a maximum value (358 ± 5°C) exhibited by Me13–43(20 k) having around 50% each of (Me-*ω*-OHC9) and (Me-*ω*-OHC13) comonomer units. The ester group concentration, C_e (Table II) for copolyesters varied only slightly with composition, i.e., from 13% for Me13–94(33 k) to 16% for Me13–43(20 k). The composition dependence of $T_{d(5)}$ for P(−Me13−/−Me9−)s is attributable to the randomization effect by the ester groups up on copolymerization.

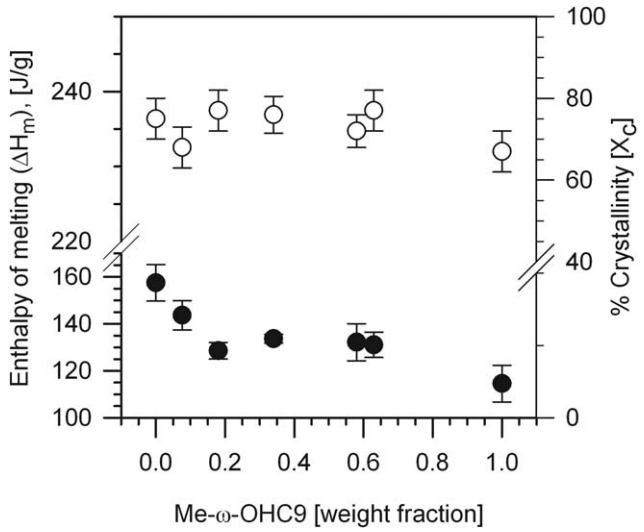

Figure 4. The composition dependence of degree of crystallinity (X_c (%)), estimated from WAXD) (○) and enthalpy of melting (ΔH_m, determined from DSC data) (●) for P(−Me13−/−Me9−) copolyesters.

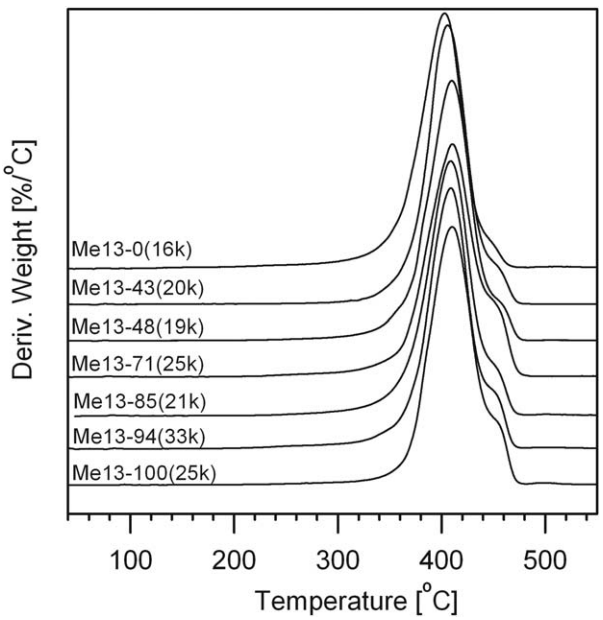

Figure 5. DTG traces of the Me9 (Me13–100(25 k)) and Me13 (Me13–100(25 k) homopolymers, and of the P(−Me13−/−Me9−) (Me13–94(33 k) to Me13–43(20 k)) copolymers obtained with heating rate of 10°C/min.

Table IV. Glass Transition Temperature (T_g) Obtained from DMA, Onset Temperature of Degradation Determined at 5% Weight Loss from TGA, $T_{d(5)}$, and Peak Decomposition Temperature ($T_{d(max)}$) Obtained from the DTG Curves for P(−Me13−/−Me9−) Copolymers

Sample code	$T_{d(5)}$ (±5°C)	$T_{d(max)}$ (±5°C)	T_g (±2°C)
Me13-100(25k)	345	412	−25.6
Me13-94(33k)	345	409	−28.8
Me13-85(21k)	350	410	−31.5
Me13-71(25k)	350	411	−32.9
Me13-48(19k)	352	410	−35.7
Me13-43(20k)	358	406	−36.2
Me13-0(16k)	324	403	-

Mechanical and Dynamic Mechanical Properties of Copolyesters

Viscoelastic response, obtained by DMA, was used to classify the glass transition temperature of the co-polyesters. Figure 7 displays the tan δ versus temperature curves for Me13–100 (25 k) homopolymer and the P(−Me13−/−Me9−) (Me13–94 (33 k) to Me13–43(20 k)) copolyesters. The Me9 (Me13-0 (16 k)) homopolymer was too brittle to prepare good test specimens. Loss (E'') and storage (E') modulus curves of the samples are shown in Supporting Information Figures S1 and S2. DMA analysis of the copolyesters revealed a sharp single glass transition marked by an abrupt decrease of ~3 GPa in elastic modulus observable between −50 and 0°C (Supporting Information Figure S2) as well as pronounced peaks in loss modulus (Supporting Information Figure S1) and tan δ (Figure 7) curves. The glass transition temperature (T_g) of the copolyesters determined from the peak value of tan δ curves are listed in Table IV. The T_g of copolyesters are in the range of −36 to −25°C (Table IV) indicating that the amorphous regions remain in the ductile state at temperatures very favorable for a large set of high end applications, especially at service temperatures which are required for biomedical polymers.[22] The T_g of P(−Me13−/−Me9−) co-polyesters decreased with increasing (Me-ω-OHC9) comonomer content (Figure 8). Contrary to the neatly packed crystalline domains, where an increasing ester group density would lead to stronger interactions, the adjacent chains only rarely come close enough in the random coils of

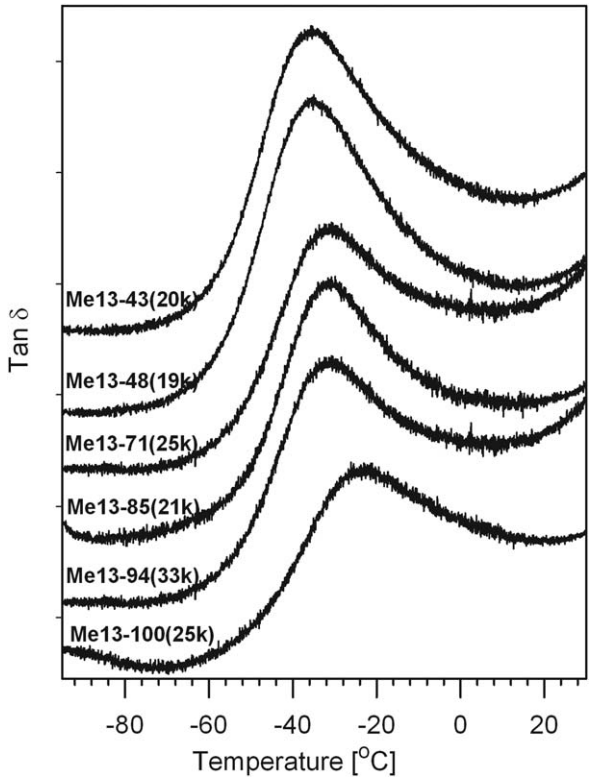

Figure 7. Tan δ versus temperature curves for (Me13–100(25 k)) homopolymer and P(−Me13−/−Me9−) (Me13–94(33 k) to Me13–43(20 k)) copolyesters.

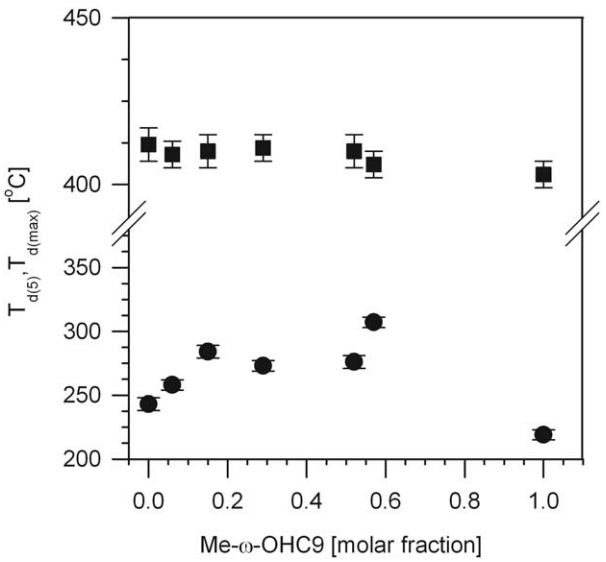

Figure 6. Composition dependence of the onset ($T_{d(5)}$) (●) and the maximum $T_{d(max)}$ degradation temperature (■) for P(−Me13−/−Me9−) copolymers.

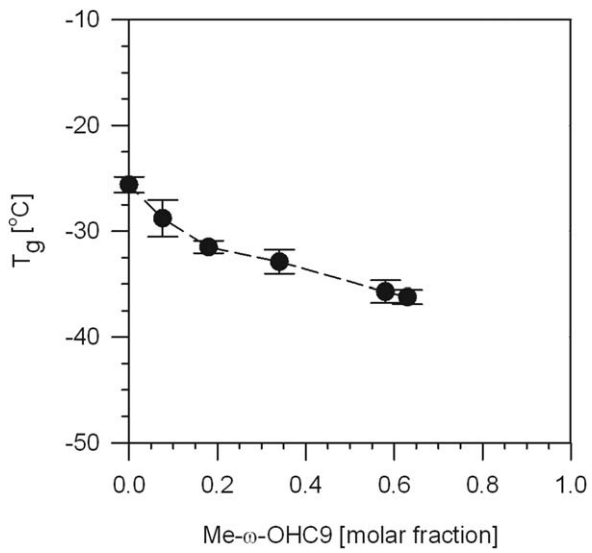

Figure 8. Composition dependence of T_g (°C) for P(−Me13−/−Me9−) copolyesters. The dotted lines are guidelines for eyes.

Table V. Physical Properties of Selected Copolyesters: Copolymer Composition Determined by ^{1}H-NMR, Number Average (M_w), Weight Average (M_n) Molecular Weights and PDI for the Compression Molded Polymers Determined by GPC

Sample code	Me-ω-OHC13/ Me-ω-OHC9 molar ratio (from ^{1}H-NMR)	M_w (g/mol)	M_n (g/mol)	PDI	X_c, (±5%)	T_g (±2°C)	TS (±1.5 MPa)	E (±50 MPa)	EB (±1%)
Me13-100(72k)	100 : 00	72,604	28,470	2.5	51	−27.8	16.3	693	5.9
Me13-71(68k)	71 : 29	67,717	19,492	3.5	68	−33.5	10.3	1011	2.4
Me13-0(72k)	00 : 100	72,147	30,377	2.4	55	−26.8	18.4	772	4.1

T_g obtained from DMA, X_c, estimated from WAXD, elongation at break (EB), ultimate strength (TS), and Young's modulus (E) obtained from tensile analysis.

the amorphous copolymer and therefore do not significantly increase the interactions between the amorphous chain segments. Instead, the increase of (O)C—O bonds in the amorphous segments increases chain flexibility, and thus decreases the T_g.[23]

The molecular weight (M_n = 9000–18,000 g/mol) of P(−Me13−/−Me9−) copolyester samples (Me13–100(25 k) to Me13-0(16 k), Table II) were not sufficient enough to make films suitable for tensile testing. Moldable dumbbell-shaped films of high molecular weight Me13 (Me13–100(72 k)), Me9 (Me13-0(72 k)) homopolymers and P(−Me13−/−Me9−) (Me13–71(68 k)) copolyester were therefore prepared and investigated for the mechanical properties (Table V).

The stress–strain curves for Me13–100(72 k), Me13-0(72 k) homopolymers and Me13–71(68 k) copolyester are provided in the Supporting Information in Figure S3, and the corresponding stress–strain results are listed in Table V. As can be seen in Table V, the copolyester presented the highest Young's modulus (1011 MPa) followed by Me13-0(72 k) (772 MPa) and Me13–100(72 k) (693 MPa). This trend can be explained by the degrees of crystallinity of the polymers.[24–26] As listed in Table V, X_c of Me13–71(68 k) copolyester was higher than that of Me13–100(72 k) and Me13-0(72 k) homopolymers (X_c = 68, 51 and 55%, Table V) in agreement with the variation of Young's modulus. Note that such Young's modulus values combined with the low T_gs (between −25 and −36°C) presented by the homopolymers and the copolymer indicate a ductile behavior.

Me13–100(72 k) and Me13-0(72 k) homopolymers, and Me13–71 (68 k) copolyester presented % elongation at break (EB) of less than 6% (Table V). These values are lower than what is expected for a typical ductile polymer that has T_g and M_W values comparable with those measured for the polymers. The degradation of the materials during the compression molding experiment is ruled out as the molecular weight measured before and after compression molding for these polymers was significantly statistically the same (Table V). Furthermore, DSC and TGA did not reveal any difference in the thermal behavior or thermal stability of the polymers before and after compression molding. Such low EB values can be explained by the fairly high crystallinity observed for these polymers (X_c = 55–70%, Table V). At this level of crystallinity, the number of interlamellar connections (amorphous tie molecules) available for transmitting forces between the rigid crystallites is not large enough to sustain a high elongation at break, and explains the poor toughness of these materials.[27]

CONCLUSIONS

The effect of composition on the physical properties of vegetable-oil based Poly(ω-hydroxy nonanoate/ω-hydroxy tridecanoate) P(−Me13−/−Me9−) random copolyesters (M_n = 11,000–18,500 g/mol) were investigated using WAXD, DSC, DMA TGA, and tensile analysis. P(−Me13−/−Me9−) adopted a polyethylene-like orthorhombic crystalline packing over the whole composition range. The melting, glass transition and thermal decomposition behavior of P(−Me13−/−Me9−)s varied with composition. Their crystallinities however, showed very little variability with copolyester composition. The copolyester exhibited highest Young's modulus followed by the homopolymers and was explained in relation to their degrees of crystallinity. These thermally stable thermoplastics are excellent examples of aliphatic polyester systems that can be tuned by varying the density of degradable ester groups (by varying the composition) without any drastic impact on crystallinity and related physical properties.

ACKNOWLEDGMENTS

The financial support of Elevance Renewable Sciences, NSERC, Grain Farmers of Ontario, GPA-EDC, Industry Canada, and Trent University is gratefully acknowledged.

REFERENCES

1. Philip, S.; Keshavarz, T.; Roy, I. *J. Chem. Technol. Biotechnol.* **2007**, *82*, 233.
2. Martin, D. P.; Williams, S. F. *Biochem. Eng. J.* **2003**, *16*, 97.
3. Kumar, S.; Prakashl, N.; Dattaz, D. *Biopolym.: Biomed. Environ. Appl.* **2011**, *70*, 169.
4. Zhang, D.; Hillmyer, M. A.; Tolman, W. B. *Macromolecules* **2004**, *37*, 8198.
5. Labet, M.; Thielemans, W. *Chem. Soc. Rev.* **2009**, *38*, 3484.
6. Kim, E.; Uyama, H.; Doi, Y.; Ha, C.-S.; Iwata, T. *Macromol. Biosci.* **2005**, *5*, 734.
7. Trzaskowski, J.; Quinzler, D.; Bahrle, C.; Mecking, S. *Macromol. Rapid Commun.* **2011**, *32*, 1352.

8. Li, X.; Sun, J.; Huang, Y.; Geng, Y.; Wang, X.; Ma, Z.; Shao, C.; Zhang, X.; Yang, C.; Li, L. *Macromolecules* **2008**, *41*, 3162.
9. Petrovic, Z. S.; Milic, J.; Xu, Y. J.; Cvetkovic, I. *Macromolecules* **2010**, *43*, 4120.
10. Jose, J.; Pourfallah, G.; Merkley, D.; Li, S.; Bouzidi, L.; Leao, A.; Narine, S. S. *Polym. Chem.* **2014**, DOI:10.1039/c3py01261a.
11. Jose, J.; Pourfallah, G.; Li, S.; Bouzidi, L.; Leao, A. L.; Narine, S. S. *Biomacromolecules* **2014**, DOI:10.1002/pi.4714.
12. Jeong, Y.; Jo, W.; Lee, S. *Macromol. Res.* **2004**, *12*, 459.
13. Jeong, Y. G.; Jo, W. H.; Lee, S. C. *Macromolecules* **2003**, *36*, 4051.
14. Liang, Z.; Pan, P.; Zhu, B.; Dong, T.; Hua, L.; Inoue, Y. *Macromolecules* **2010**, *43*, 2925.
15. Bero, M.; Czapla, B.; Dobrzynski, P.; Janeczek, H.; Kasperczyk, J. *Macromol. Chem. Phys.* **1999**, *200*, 911.
16. Ceccorulli, G.; Scandola, M.; Kumar, A.; Kalra, B.; Gross, R. A. *Biomacromolecules* **2005**, *6*, 902.
17. Murthy, N.; Minor, H. *Polymer* **1990**, *31*, 996.
18. Allegra, G.; Bassi, I. W. In: Fortschritte der Hochpolymeren-Forschung; Schonberg, A., Ed.; Springer-Verlag: New York, USA, **1969**, Chapter 3, p 549.
19. Wunderlich, B. In Macromolecular Physics-Crystal Structure, Morphology, Defects; Academic Press: New York, **1973**, p 147.
20. Bunn, C. W. *Trans. Faraday Soc.* **1939**, *35*, 482.
21. Piotr, K. *Prog. Mater. Sci.* **2007**, *52*, 915.
22. Ratner D. Buddy, H. S. A.; Frederick, S. J.; Jack, L. E. Biomaterials Science—An Introduction to Materials in Medicine; Academic Press: London, UK, **1996**.
23. Brydson, J. A. In Plastics Materials, 7th ed.; Brydson, J. A., Ed.; Butterworth-Heinemann: Oxford, **1999**, p 59.
24. Kennedy, M. A.; Peacock, A. J.; Mandelkern, L. *Macromolecules* **1994**, *27*, 5297.
25. Mandelkern, L. *Accounts Chem. Res.* **1990**, *23*, 380.
26. Capaccio, G.; Crompton, T. A.; Ward, I. M. *J. Polym. Sci.: Polym. Phys. Ed.* **1976**, *14*, 1641.
27. Peacock, A. In Handbook of Polyethylene: Structures: Properties, and Applications; Marcel Dekker: New York, **2000**, p 451.